On the present and future economic viability of stand-alone pressure-retarded osmosis

Citation: Chung, Hyung Won, Leonardo D. Banchik, Jaichander Swaminathan, and John H. Lienhard V. "On the Present and Future Economic Viability of Stand-Alone Pressure-Retarded Osmosis." Desalination 408 (April 2017): 133–144.

As Published: http://dx.doi.org/10.1016/j.desal.2017.01.001

Publisher: Elsevier B.V.

Persistent URL: http://hdl.handle.net/1721.1/107716

Version: Author's final manuscript: final author's manuscript post peer review, without publisher's formatting or copy editing

On the present and future economic viability of stand-alone pressure-retarded osmosis

Hyung Won Chung, Leonardo D. Banchik, Jaichander Swaminathan, John H. Lienhard V*

Rohsenow Kendall Heat Transfer Laboratory, Department of Mechanical Engineering, Massachusetts Institute of Technology, Cambridge MA 02139-4307 USA

Abstract

Pressure-retarded osmosis is a renewable method of power production from salinity gradients which has generated significant academic and commercial interest but, to date, has not been successfully implemented on a large scale. In this work, we investigate lower bound cost scenarios for power generation with PRO to evaluate its economic viability. We build a comprehensive economic model for PRO with assumptions that minimize the cost of power production, thereby conclusively identifying the operating conditions that are not economically viable. With the current state-of-the art PRO membranes, we estimate the minimum levelized cost of electricity for PRO of US$1.2/kWh for seawater and river water pairing, $0.44/kWh for reverse osmosis brine and wastewater, and $0.066/kWh for nearly saturated water (26% wt) and river water, all for a 2 MW production system. Only a pairing of extremely high salinity (greater than 18%) water and freshwater has the potential to compete with wind power currently at $0.074/kWh. We show two methods for reducing this cost via economies of scale and reducing the membrane structural parameter. We find that the latter method reduces the levelized cost of electricity significantly more than increasing the membrane permeability coefficient.

Keywords: Pressure-retarded osmosis; Economic analysis; Levelized cost of electricity (LCOE); Renewable energy; High salinity

H.W. Chung, L.D. Banchik, J. Swaminathan, and J.H. Lienhard V, "On the present and future economic viability of stand-alone pressure-retarded osmosis," *Desalination*, **408**:133-144, 15 April 2017.

*Corresponding author: lienhard@mit.edu

1. Introduction

While the consequences of climate change are becoming increasingly felt globally, renewable sources of energy such as solar and wind power are being adopted at rapidly accelerating rates. This is predominantly due to drastic cost reductions which allowed these technologies to attain grid parity, or compete economically with retail rates of grid power by fossil fuels [1, 2]. In 1955, Pattle [3] wrote that an untapped potential source of exergy is lost when seawater is mixed with river water and proposed a system for recovering this lost resource. About two decades later, Loeb invented two practical methods, pressure-retarded osmosis (PRO) and reverse electrodialysis (RED), to harness this untapped source of energy which involves the controlled mixing of two streams with different salinities [4, 5] such as river water and seawater or desalination brine and treated municipal wastewater. While RED has been extensively studied from both energetic and economic point of views [6, 7, 8], PRO has been found to have a higher energy efficiency and power density than RED [9].

PRO has received substantial attention in the academic literature recently [10, 11, 12] and several researchers have studied integrating PRO with reverse osmosis systems to reduce the overall energy consumption for desalination [13, 14]. But these studies were focused solely on energetic analyses of PRO and fewer studies have investigated the economic viability of this technology. However, just as attaining grid parity enabled and continues to enable widespread adoption of solar photo-voltaic and wind power, so too do economic considerations determine the viability of PRO systems. Given the significant academic and commercial interest in PRO, a comprehensive economic assessment is both imperative and timely.

In this study, we compute the minimum levelized cost of electricity ($\mathrm{LCOE_{min}}$) in US$/kWh and the minimum overnight cost-of-capital ($\mathrm{OCC_{min}}$) in US$/MW for a variety of draw and feed stream combinations. These figures of merit allow for a direct comparison between PRO and other energy sources including renewables, such as wind and solar, or fossil technologies, such as diesel and natural gas.

The novelty of this work lies in using lower bound cost estimates rather than attempting to precisely estimate costs. The aim therefore is to sharply characterize sets of operating conditions as economically unviable. In addition, we use a comprehensive optimization algorithm that enables exploration of a large space of operating conditions rather than being restricted to some arbitrarily set operating condition. Finally, the effect of system scale up on the economic viability is also considered. These factors are discussed in more detail in the following subsections.

Lower bound cost estimates

Firstly, we use lower bound cost estimates to determine the economic viability of stand-alone PRO. This is because accurately estimating capital cost (CapEx) and pretreatment cost data for PRO is difficult due to the lack of large scale PRO plants in existence. Previously estimated PRO system costs in the literature vary greatly due to selection of these values and it is unclear which are the most accurate. Instead of attempting to accurately determine the cost of a PRO system, we adopt simplifying assumptions whenever there is uncertainty which lead to the lowest possible cost - thereby providing a lower bound on the cost of electricity generated by PRO. One of our most important assumptions is that we use capital costs of modern seawater reverse osmosis (SWRO) plants of a similar size to estimate PRO CapEx. Although RO and PRO are similar, directly applying the RO CapEx to PRO may result in overestimation of the PRO CapEx. Whenever we believe there exists a difference between PRO and RO, we exclude the CapEx contribution from the specific item which is attributed to the difference (e.g., the intake system). We chose SWRO because the salinity of draw stream considered in this study is greater than or equal to seawater salinity. Because RO technology and construction methods are rather mature, using their capital cost should provide a lower bound cost to our PRO study.

Comprehensive model and optimization algorithm which explores a large set of process parameters

Secondly, our model is one of the most comprehensive to date due to consideration of all known loss mechanisms including internal and external concentration polarization, reverse solute flux, viscous losses in hydraulic pressure, and axial changes in concentration due to large system sizes. We also take into account the decrease in membrane permeability at high pressures (> 45 bar) due to compaction - a critical, but poorly understood factor which must especially be considered when using high osmotic pressure draw streams to produce power.

In addition to our large set of explored draw and feed stream combinations, we use a four parameter non-linear optimization method to investigate a vast range of feed and draw velocities, applied hydraulic pressures, system sizes, and mass flow rate ratios. With our lower bound cost estimation method, we can clearly rule out a large set of infeasible operating regimes. Our optimization approach makes the results from our study general rather than being limited to one choice of parameters.

While we are not the first to explore the economic viability of PRO, most studies have focused on pairing seawater with freshwater (or river water level salinity) [15, 16, 17, 18]. Kleiterp [15] investigated the commercial potential of PRO but used a zero dimensional model which does not take into account the decreasing driving force along the length of the PRO module. This choice of model significantly over-predicts the power density, which in turn results in an underestimate of the cost of electricity.

Skilhagen et al. [18] suggested that 5 W/m^2 is required for the feasibility of PRO but did not specify the details of their economic argument. Lee et al. [16] assumed a power density value and membrane cost without using a PRO model to study only the OCC. Ramon used an exceptionally low capital cost (\$234 day/m^3 of permeate), less than a quarter of the cost of a typical SWRO plant (>\$1000 day/m^3 [19]), which resulted in an electricity cost of US\$0.06/kWh.

Some papers studied solution pairings other than river water/seawater, but use unreasonable assumptions or scale-up factors that may not be accurate. Loeb [20] studied a large scale PRO plant which uses Dead Sea and RO brine as inlets and achieved US\$0.058/kWh in 1998 (US\$0.084/kWh in 2016 [21]). Loeb [22] also studied pairing 12% (by weight) salinity stream of the Great Salt Lake with nearby river water and achieved US\$0.09/kWh in 2001 (US\$0.12 kWh in 2001 [21]). However, both studies based capital cost on a brackish RO plant (\$420 day/m^3), which is less than half the cost of a SWRO plant (>\$1000 day/m^3 [19]) due to the absence of high pressure pumps in brackish water RO. Also Loeb used a scale-up cost factor which may not be accurately applied to PRO.

Future PRO economic viability

Finally, we study the future economic viability of PRO by pushing the limits of PRO membrane technology in our models. We first identify two potential methods of reducing the LCOE: harnessing economies of scale and improving membrane performance. We find that the $\mathrm{LCOE}_{\mathrm{min}}$ is reduced by 42% as the net power production is increased from 2 to 75 MW. Then we compute the $\mathrm{LCOE}_{\mathrm{min}}$ for PRO systems with up to an order-of-magnitude greater water permeability coefficient, lower solute passage, and smaller structural parameter while maintaining the salt permeability constant–all steps which have been proposed to prepare PRO for commercialization and real-world application [17, 23, 24]. We find that decreasing the structural parameter results in a more significant decrease in $\mathrm{LCOE}_{\mathrm{min}}$ than increasing the membrane permeability.

With these unique analyses, we conclusively demonstrate that PRO has potential to be economically viable only if extremely high draw salinity is used (at least above 18%). Therefore, we suggest that future PRO research be focused on challenges associated with implementing highly saline draw solutions.

2. Economic model to obtain a lower bound cost of energy from PRO

A representative PRO system is shown in Fig. 1. A counterflow[1] PRO module takes draw and feed solutions to produce power. After leaving the PRO module, the draw stream is divided into two parts. A pressure exchanger (PX) is used to transfer mechanical energy from a portion of the total outlet draw stream ($Q_{\mathrm{d,out}}$) to the incoming draw stream ($Q_{\mathrm{d,in}}$). The pressure exchanger requires equal volumetric flow rates so that $Q_{\mathrm{d,in}} = Q_{\mathrm{d,out}}$. The remainder of the draw exiting the PRO module (Q_{t}) is run through the turbine, which in turn is connected to a generator in order to produce power. A lower salinity feed stream flows on the other side of the PRO membrane. Due to a difference in chemical potential, water is drawn from the feed to the draw side via osmosis. Because the inlet draw stream is at a higher hydraulic pressure than the feed ($P_{\mathrm{d,in}} > P_{\mathrm{f,in}}$), the transmembrane osmotic driving force is retarded by the hydraulic pressure of the draw stream (i.e., pressure-retarded osmosis).

[1] We investigate counterflow exchangers as opposed to parallel flow exchangers in this work because the latter configuration produces less power irrespective of operating conditions [25].

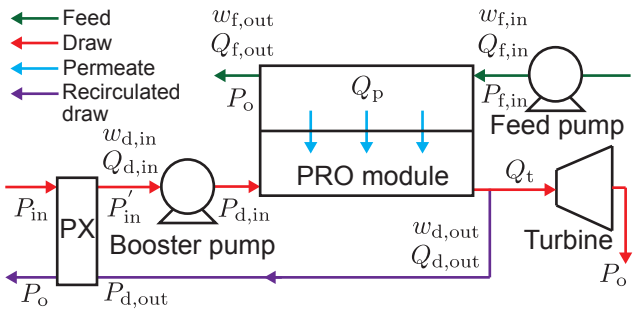

Figure 1: Flow diagram of PRO system.

2.1. Economic analysis

Two metrics are used for economic analysis: levelized cost of electricity ($LCOE_{min}$) in \$/kWh and overnight capital cost (OCC_{min}) in \$/MW. The OCC is defined as a ratio of capital cost to total power production. It quantifies the capital cost if the plant can be built overnight and does not take into account the time value of money. These up-to-date metrics for other power generation technologies are available from the U.S. Energy Information Administration [26]. By calculating LCOE and OCC for PRO, a direct comparison can be made to other technologies to assess the economic feasibility of PRO. As of 2015, wind power had the lowest national average (U.S.) values of LCOE [26] and OCC [27], apart from geothermal energy, of \$0.074/kWh and \$2.2/MW, respectively. In this paper, we use wind power as a benchmark target for comparing against PRO because of its low LCOE. Table 1 shows LCOE and OCC values for other power generation technologies.

Table 1: LCOE and OCC of power generation technologies as of 2015 [26]. CC stands for combined cycle.

Technology	LCOE [\$/kWh]	OCC [\$/MW]
Conventional coal	0.095	3.8
Natural gas (conventional CC)	0.075	0.92
Natural gas (advanced CC)	0.073	1.0
Solar PV	0.13	3.9
Onshore wind	0.074	2.2
Hydroelectric	0.084	2.9

Since very few large scale PRO plants exist, capital expenditure (CapEx) for a full PRO plant is difficult to estimate. Instead, we estimated PRO CapEx using data from reverse osmosis plants as was done by Loeb [20, 28]. While a PRO plant would be very similar to an RO plant, it is more complex because it involves two streams and requires two pumps. Therefore, in addition to the fact that RO is a rather mature and well-optimized technology, SWRO CapEx can serve as a lower limit estimate of the PRO CapEx. PRO and RO ancillary systems are also different. For example, both feed and draw solutions have to be pretreated in the case of PRO. In the PRO literature, pretreatment is not well understood [29, 30]. For our main conclusions, we neglect the energy consumption and cost of pretreatment in order to avoid introducing an additional source of uncertainty and to be consistent with our methodology of estimating the lower bound LCOE and OCC. In Sec. 3.2, however, we reintroduce pretreatment to estimate its effect on the net power production and cost.

We use SWRO CapEx data from Desaldata.com [31], which has a detailed breakdown of CapEx items (e.g., intake and outfall system, pressure vessels, etc.). Among these items, we deliberately exclude irrelevant or uncertain items (which may introduce uncertainty to the analysis). More specifically, we neglected intake and outfall system costs because these items are specific to plant location. We also neglect CapEx costs associated with pretreatment because of the uncertainty of PRO pretreatment requirements. These exclusions by themselves result in about a 16% reduction in CapEx. Pumps are not excluded because for high salinity draw streams, the operating pressure of PRO is much higher than that of RO. As will be shown in Sec. 3,

the optimum pressure fo r a0.1/26% salinity pair is 173 bar, which is more than twice the operating pressure of SWRO (approximately 70 bar).

Using the CapEx data, the membrane price per unit area can be calculated ($15–40/m^2 range). In the present work, we assume that PRO membranes can be produced for the same price as RO membranes. Because RO is a mature technology, this assumption results in significantly lower PRO costs compared to using currently available PRO membrane costs. Details on how we obtained CapEx data can be found in Appendix A.

$\mathrm{LCOE_{min}}$ is a function of both capital and operating expenditures (OpEx). OpEx includes labor, membrane replacement, chemicals, etc. In order to be consistent with the lower limit cost estimation, only membrane replacement is included in the OpEx because other items are not fully understood or may vary greatly for PRO application. The detailed economic analysis framework can be found in Appendix A. The $\mathrm{LCOE_{min}}$ and $\mathrm{OCC_{min}}$ can be calculated as follows:

$$\mathrm{LCOE_{min}} = \frac{\mathrm{CapEx} \cdot \mathrm{CRF}}{\dot{W}_{\mathrm{net}} t_{\mathrm{op}}} + \frac{C_{\mathrm{m}} A_{\mathrm{m}}}{L_{\mathrm{m}} \dot{W}_{\mathrm{net}} t_{\mathrm{op}}} \tag{1}$$

$$\mathrm{OCC_{min}} = \frac{\mathrm{CapEx}}{\dot{W}_{\mathrm{net}}} \tag{2}$$

where CRF is the capital recovery factor, $\dot{W}_{\mathrm{net}}$ is the net power production from PRO, t_{op} is the annual operation time, C_{m} is the cost of membrane per unit membrane area, and A_{m} is the membrane area. $\dot{W}_{\mathrm{net}}$ is defined as the difference between the total power produced by the turbine and generator ($\dot{W}_{\mathrm{PRO}}$) and the pumping power as shown in Eq. (3):

$$\dot{W}_{\mathrm{net}} = \dot{W}_{\mathrm{PRO}} - \dot{W}_{\mathrm{pump}} \tag{3}$$

2.2. Optimization methodology

A commercial forward osmosis (FO) membrane from Hydration Technology Innovation was used as the basis for membrane properties. Straub et al. [32] investigated this membrane and reported that $A = 2.49$ L/m^2-hr-bar, $B = 0.39$ L/m^2-hr and $S = 564$ µm, where A is the membrane pure water permeability coefficient, B is the solute permeability coefficient, and S is the structural parameter. The structural parameter is a function of the porosity, tortuosity, and thickness of the membrane support layer.

In PRO, the power production $\dot{W}_{\mathrm{PRO}}$ is a function of the inlet salinities of the feed ($w_{\mathrm{f,in}}$) and draw ($w_{\mathrm{d,in}}$) streams, the membrane area (A_{m}), the inlet velocity of either stream (v), the dimensionless pressure on the draw stream (P^*), and the mass flow rate ratio (MR) as specified by Eq. (4)

$$\dot{W}_{\mathrm{PRO}} = f\left(w_{\mathrm{f,in}},\, w_{\mathrm{d,in}},\, A_{\mathrm{m}},\, v,\, P^*,\, \mathrm{MR}\right) \tag{4}$$

where the dimensionless net draw pressure and MR are defined, respectively, as [25]:

$$P^* = \frac{P_{\mathrm{d,in}} - P_{\mathrm{f,in}}}{\pi_{\mathrm{d,in}} - \pi_{\mathrm{f,in}}} \tag{5}$$

$$\mathrm{MR} = \frac{\dot{m}_{\mathrm{d,in}}}{\dot{m}_{\mathrm{f,in}}} \tag{6}$$

The denominator of Eq. (5) is the maximum osmotic pressure difference. The total power ($\dot{W}_{\mathrm{PRO}}$) can be used to calculate the levelized cost of electricity ($\mathrm{LCOE_{min}}$) as discussed in Sec. 2.1. The inlet salinities of the two streams are specified as inputs for each case study. The remaining four independent variables (A_{m}, v, P^*, and MR) are determined such that LCOE is minimized, through non-linear optimization over a wide parametric space, by the Conjugate Gradient Method using Engineering Equation Solver [33]. It is sufficient to specify only the velocity of either the draw or feed stream because the velocity of the other stream can be determined by conservation of mass and MR. The computational flow for our optimization scheme is shown in Fig. 2. As we will discuss in the next section, the only parameter that is specified as a constant is the channel height (h). Our choice of h, however, is appropriate assuming that PRO will use channel heights and spacers that are common to the RO industry. Because the independent variables are specified through

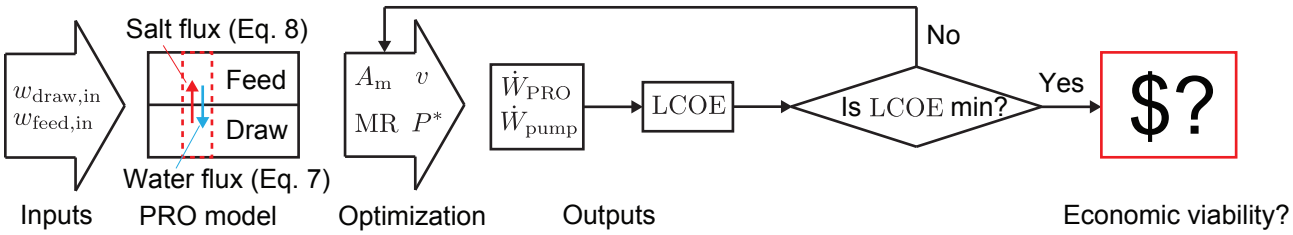

Figure 2: Computational flow for optimization algorithm to find $\mathrm{LCOE}_{\mathrm{min}}$ and determine economic viability of PRO.

optimization, the results of the simulation do not depend on a particular choice of operating condition. To the authors' knowledge, this extent of generality has not been previously achieved in the PRO literature.

Table 2 qualitatively shows the first order effects of the four independent variables.

Table 2: Qualitative effect of independent variables.

	Too low	Too high
A_{m}	Low energy generation	High CapEx
v	High concentration polarization	High pumping power
MR	High pumping power for feed	High pumping power for draw
P^*	Small turbine power	Small flux

We can infer the presence of a global minimum by studying the limiting behaviors of the four independent variables. As each variable approaches zero or positive infinity (unity for P^* because it is a dimensionless variable defined from zero to unity), the power production and resulting $\mathrm{LCOE}_{\mathrm{min}}$ approach zero or infinity, respectively. For example, when P^* approaches zero, the draw stream at the turbine inlet is not pressurized to produce any power. Likewise when P^* approaches unity, flux ceases and power production approaches zero.

2.3. Numerical model based on finite difference method including comprehensive list of loss mechanisms

The PRO module is discretized into a number of computational cells and transport equations were solved for each cell using Engineering Equation Solver [33] which is a simultaneous equation solver. Equation (7) describes how permeate flux (J_{w}) is calculated, at each position x, along the axial flow direction by the solution diffusion model:

$$J_{\mathrm{w}}(x) = A\left\{\pi_{\mathrm{d,m}}(x) - \pi_{\mathrm{f,m}}(x) - \left[P_{\mathrm{d}}(x) - P_{\mathrm{f}}(x)\right]\right\} \tag{7}$$

where $\pi_{\mathrm{d,m}}$ and $\pi_{\mathrm{f,m}}$ are the draw and feed osmotic pressures at the membrane surface (to account for concentration polarization), and P is the hydraulic pressure of each stream at an axial position x. Equation (8) describes how reverse salt flux is calculated for Fickian diffusion:

$$J_{\mathrm{salt}}(x) = B\rho\left[w_{\mathrm{d,m}}(x) - w_{\mathrm{f,m}}(x)\right] \tag{8}$$

where ρ is the density (approximated as that of pure water), and $w_{\mathrm{d,m}}$ and $w_{\mathrm{f,m}}$ are the solute mass fractions[2] at the membrane on the draw and feed side. Two implicit equations for concentration polarization (Eqs. (9) and (10)) are used to calculate $w_{\mathrm{d,m}}$ and $w_{\mathrm{f,m}}$ using the bulk feed and draw salinities, the external mass transfer coefficient k on the draw side, and membrane support layer properties.

$$w_{\mathrm{d,m}} = w_{\mathrm{d,b}}\exp\left(-\frac{J_{\mathrm{w}}}{\rho k}\right) - \frac{B\left(w_{\mathrm{d,m}} - w_{\mathrm{f,m}}\right)}{J_{\mathrm{w}}}\left[1 - \exp\left(-\frac{J_{\mathrm{w}}}{\rho k}\right)\right] \tag{9}$$

[2]Our transport model considers mass-based rather than volume-based salinity because volume is not conserved.

$$w_{\mathrm{f,m}} = w_{\mathrm{f,b}} \exp\left(\frac{J_{\mathrm{w}} S}{\rho D}\right) + \frac{B\left(w_{\mathrm{d,m}} - w_{\mathrm{f,m}}\right)}{J_{\mathrm{w}}} \left[\exp\left(\frac{J_{\mathrm{w}} S}{\rho D}\right) - 1\right] \tag{10}$$

The diffusion coefficient, D, of NaCl as a function of salinity was tabulated by Robinson and Stokes [34]. It varies between 1.474×10^{-9} and 1.62×10^{-9} m^2/s over the salinity range of 0 to 22.6 % at temperature of 25°C. Because of the small variation, an average value of 1.52×10^{-9} m^2/s was used.

Simultaneously solving local transport equations (Eqs. (7) and (8)) at all x locations completely specifies the PRO system. From this, other parameters of interest such as power production can be calculated. Our model includes a comprehensive set of loss mechanisms including external and internal concentration polarization, reverse salt flux, viscous pressure drop, and membrane compaction. A detailed description of the model can be found in Appendix B.

3. Results and discussion

3.1. Energetic optimum and economic optimum are dramatically different

Many researchers have focused on energetic analysis of PRO, as discussed in Sec. 1. While energetic analysis is crucial to understand the theoretical basis of PRO and the limits of power production, the most relevant metric needed for the widespread adoption of PRO technology (or any other energy technology) is its cost.

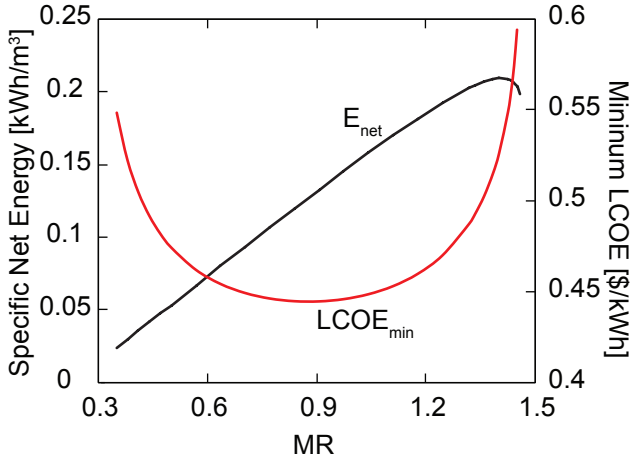

Figure 3: Energetic and economic optima for 0.1/7% (river water or treated wastewater effluent and desalination brine) salinity pair as a function of the draw to feed mass flow rate ratio, MR. The net power output is fixed at 2 MW.

Figure 3 shows the effect of varying the mass flow rate ratio (MR) on the specific net energy production (i.e., $E_{\mathrm{net}} = E_{\mathrm{PRO}} - E_{\mathrm{pump}}$) and $\mathrm{LCOE}_{\mathrm{min}}$. Note that we use E to denote the rate of energy transfer normalized by the feed flow rate and $\dot{W}$ to denote the non-normalized energy transfer rate. The optima are drastically different. Thermodynamically, a larger membrane area is required to reduce the irreversible losses. However, larger membrane areas increase system size and, therefore, CapEx. Because of these opposing effects, energetic optimum and economic optimum are usually different for typical energy systems. Figure 3 shows that PRO follows this trend as well. Although Fig. 3 is generated using net energy production normalized by the feed volumetric flow rate, the same trend is observed even if it is normalized by the draw or combined feed and draw volumetric flow rate. It is unreasonable to increase the energy production and efficiency by increasing the cost of electricity. Therefore, energetic analysis cannot be used to judge viability of PRO, and economic analysis is indispensable. The subsequent sections focus on economic analysis.

3.2. Increasing draw salinity drastically reduces the cost

Recalling Eq. (4), four independent variables are used for optimization, leaving two independent variables (i.e. salinities of feed and draw streams) which can be used as inputs for a parametric study. It can be shown

that a low salinity feed stream should be used to maximize power production. Detailed analysis can be found in Appendix D. Throughout the paper, we hold the feed salinity at 0.1% to keep it as low as possible while still retaining practicality. This value represents the salinity of typical treated wastewater effluent (TWE) or river water. In this section, the draw salinity is varied from seawater level to NaCl saturation (26%), and the effect of draw salinity on $LCOE_{min}$ and OCC_{min} is studied. In practice, a pretreated stream at 26% salinity would rarely be available for use. Therefore, 0.1/26% pairing is a hypothetical situation that serves as a minimum cost case.

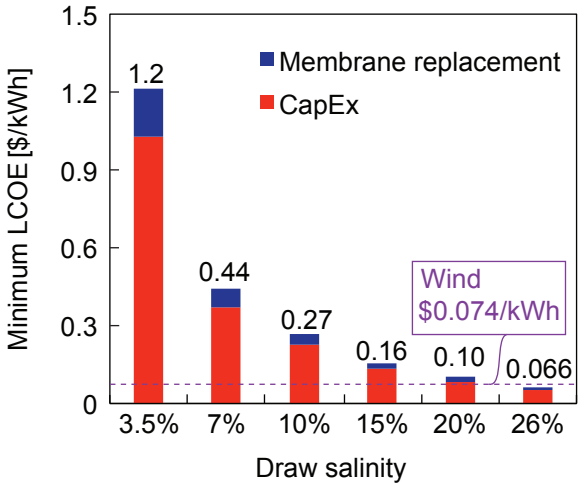

Figure 4: Effect of draw stream salinity on $LCOE_{min}$. The feed salinity is 0.1% for all cases and the net power output is held constant at 2 MW. Wind LCOE ranges from \$0.066/kWh to \$0.082/kWh, and the U.S. national average value [26] corresponds to \$0.074/kWh.

Figure 4 shows the $LCOE_{min}$ for various salinity pairs as well as the cost breakdown. The net power output is 2 MW in each case, which is enough power for roughly 607 American homes [35]. The most common salinity pairs studied in literature such as river water/seawater (0.1/3.5%) and river water/RO brine(0.1/7%) have an $LCOE_{min}$ of about 15 and 6 times higher than that of wind power[3], respectively. Only for the extreme salinity pair (0.1/26% pair) is the $LCOE_{min}$ comparable to the LCOE of wind. While CapEx is the dominant cost factor, it decreases with increasing draw salinity due to a reduction in the required membrane area when the driving force is increased. At 2 MW net power output, the $LCOE_{min}$ matches that of wind at draw salinity of 24.1%. Even if the membrane replacement cost is neglected, the $LCOE_{min}$ of PRO is still higher than that of wind except for the 0.1/26% pair, again confirming that energetic considerations alone cannot determine the feasibility of PRO.

Another economic metric of interest is overnight capital cost (OCC). Figure 5 shows the effect of varying draw salinity on OCC_{min}. The OCC_{min} for all combinations of salinity is higher than that of wind (\$2.2/MW). Recalling that these calculations embed many assumptions that lower the cost and that there is no available 26% pretreated stream, we conclude that standalone PRO cannot compete with wind power in terms of OCC. Comparison of Fig. 4 and 5 shows that $LCOE_{min}$ and overnight capital cost have a similar functional dependence on the draw salinity. Therefore, we focus on $LCOE_{min}$ in the subsequent sections.

3.3. Relative energetic cost of pretreatment decreases with increasing draw salinity

So far, pretreatment has been neglected because it may potentially introduce significant uncertainty to our analysis. By including the pretreatment, we can deduce important conclusions by comparing the relative impact of pretreatment on two different salinity pairs. Straub et al. [29] suggest a range of pretreatment energy consumption values from RO practice: 0.05-0.2 kWh/m^3 for feed and 0.1-0.4 kWh/m^3 for draw. We

[3]Wind power was chosen as a benchmark because it was the second cheapest renewable technology. The first is geothermal but only limited capacity is available at the projected lowest LCOE.

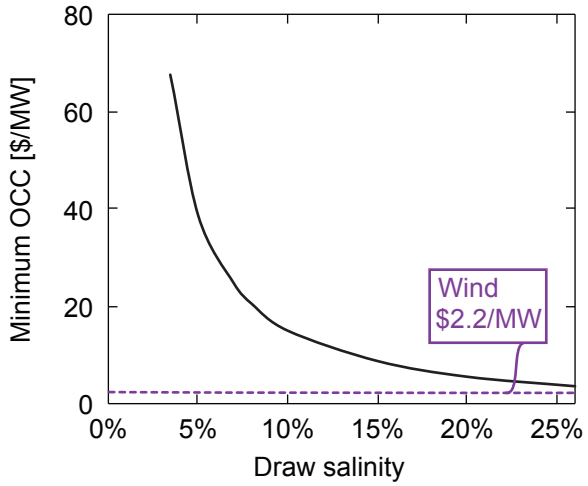

Figure 5: Effect of draw salinity on the overnight capital cost. Feed salinity was fixed at 0.1% and the net power output is 2 MW.

chose 0.05 and 0.1 kWh/m^3 for the feed and draw streams, respectively, for the 0.1/7% salinity pair. In order to account for the fact that more pretreatment may be needed for the 26% draw stream, 0.4 kWh/m^3 was used. This pretreatment energy consumption was subtracted from total power production to calculate the net power ($\dot{W}_{\text{net}} = \dot{W}_{\text{PRO}} - \dot{W}_{\text{pump}} - \dot{W}_{\text{pretreatment}}$).

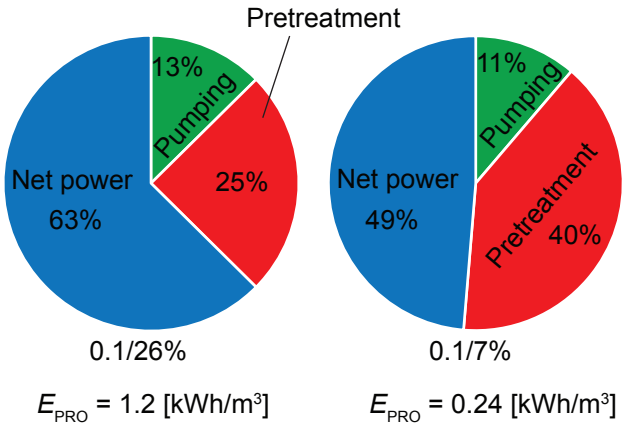

Figure 6: Energy breakdown for 0.1/26% and 0.1/7% salinity pairs. For the 0.1/7% pair, pretreatment constitutes a larger proportion of the total power production. Specific energy (E_{PRO}) is the total power production normalized by the feed.

Figure 6 shows how total power produced is divided for 0.1/26% and 0.1/7% salinity pairs. We do not include a 0.1/3.5% pair because our energetic model results in a negative net power production when pretreatment energies are included, as found by other researchers [29]. Because less power is produced for the 0.1/7% salinity pair, the pretreatment requirement contributes to a larger fraction of the total power. Practically, this means that an operator has more flexibility in choosing the draw stream source when higher salinities are used. But the absolute amount of pretreatment energy is still higher for the case of higher draw salinity because E_{PRO} is higher. It is important to note that using different numerical values for the pretreatment energy requirement results in a similar trend. Therefore, the general conclusion of this section is not dependent on the particular values of pretreatment energetics.

3.4. The highest operating pressure can be reduced without significantly increasing $LCOE_{min}$, but maximum flux increases above the critical flux

The results of Sec. 3.2 suggest that an extremely high draw salinity (e.g., 0.1/26% pair) be used. However, engineering challenges remain unresolved for utilizing a high draw salinity. One major issue is scaling and fouling. Scaling occurs when salts precipitate from saturated draw solutions close to the inlet and would be exacerbated by high fluxes which lead to high concentration polarization. Fouling occurs if highly saline draw solutions also contain a considerable amount of total suspended solids and/or biological material and is also worsened by high fluxes. In order to be consistent with other assumptions that result in lower limit LCOE, we neglect the effect of scaling and fouling. This ensures that the resulting LCOE is a lower bound because in reality these two phenomena reduce membrane permeabilities over time and adversely affect transport processes. Another major problem is the fact that the hydraulic pressure on the draw side needs to be extremely high to reduce cost. This is because osmotic pressure is high; the osmotic pressure at 26% NaCl salinity is about 380 bar. The resulting optimal draw inlet pressure is 178 bar (or about 47% of the maximum osmotic pressure difference) for a 0.1/26% salinity pair. The issue is that current commercial RO membranes are only rated to withstand maximum operating pressures of 69-83 bar [36, 37, 38, 39]. In this section, we investigate the economic penalty of lowering the draw side hydraulic pressure to pressures recommended by membrane manufacturers. Figure 7 shows the $LCOE_{min}$ as a function of the pressure at the draw inlet, which is the highest pressure in the system.

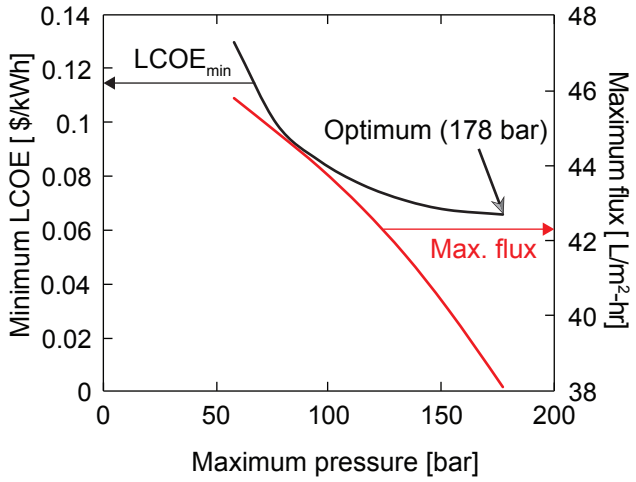

Figure 7: Effect of the top pressure on $LCOE_{min}$ and resulting local maximum flux for 0.1/26% salinity pair. The net power output is fixed at 2 MW.

Because pressure is specified as an input, each data point in Fig. 7 was obtained by optimizing three independent variables (A_m, v and MR) instead of four. When pressure is lowered from the optimal point marked in Fig. 7, the extent of flux retarding decreases and overall recovery increases while net power production at the turbine decreases because of reduced pressure. Moreover, the increase in flux results in increased concentration polarization (CP), which is an exponential function of flux. Overall, the effect of reduction in turbine power and increase in CP dominates that of increased recovery. Hence, $LCOE_{min}$ increases with a decrease in top pressure. When the pressure is decreased from 178 bar to 83 bar (53% reduction), $LCOE_{min}$ increased from \$0.066/kWh to \$0.094/kWh (43% increase) and the maximum flux increases from 38.1 to 44.6 L/m^2-hr (17% increase) for a 2 MW plant.

As shown in Fig. 7, the local maximum flux level becomes quite high (above 40 L/m^2-hr). In fact, this is higher than the typical maximum flux of 39 L/m^2-hr in RO [40]. This heuristic for upper bound flux in RO systems exists because severe fouling tends to occur above this flux level [40]. This benchmark value is a rough number that depends on a number of factors such as size of particles, feed composition and concentration, mass transfer coefficient, and velocities. Moreover, because the nature of concentration polarization is different between PRO and RO, the same benchmark for the maximum flux may not apply.

Therefore, experimental studies are needed to determine whether flux levels above 40 L/m^2-hr does or does not result in severe fouling.

3.5. A closer look at the optimization

As discussed in Sec. 2.2, the LCOE_{min} is minimized over four independent variables listed in Table 2 (A_{m}, v, MR, and P^*). Because the LCOE_{min} is calculated through optimization, the result is not constrained to an arbitrary choice of operating conditions. Studying the range of independent variables resulting from the optimization can provide further insight into PRO design and operating conditions which result in economic viability. Table 3 summarizes the range of independent and dependent variables resulting from the optimization process. As shown in Table 3, the membrane length ranges from 5 to 7.3 m whereas membrane

Table 3: Observed range of operating conditions resulting from the nonlinear optimization. This range is for the data in Section 3.2 and Appendix E and

		Observed range	
	Unit	Minimum	Maximum
A_{m}	$(\text{km})^2$	0.02	0.75
L	m	5.0	7.3
J_{min}	L/m^2-hr	11.5	27.5
J_{max}	L/m^2-hr	16.4	38.1
J_{avg}	L/m^2-hr	13.9	33.1
v	cm/s	7.5	38.3
MR	-	0.95	1.24
P^*	-	0.47	0.51
ε	-	0.28	0.39

area is on the order of km^2. This implies that the economically optimized geometry of a PRO system is a large number of relatively short modules arranged in a parallel manner. Although the flux range is not constrained in the optimization, the typical resulting fluxes are similar to operating conditions found in RO systems [41]. This is because of the exponential relationship between concentration polarization and flux: if flux is increased indefinitely, concentration polarization increases exponentially, eventually lowering the power production. The velocity range is similar to what is found in RO [41]. We also find that MR ranges around a value of unity. As discussed in Table 2, MR values far greater or lesser than unity increase the pumping power of one stream relative to other. Lastly, the optimal dimensionless pressure ratio, surprisingly, is approximately 0.5. This should be differentiated from the widely used optimum P^* value of 0.5 [17, 16, 15]. Banchik et al. [25] found that this result only applies to zero-dimensional system where virtually no stream-wise variation of properties exist, and that P^* values that optimize a module scale system (one-dimensional) are significantly different. These previous works were based on an energetic perspective, however. In this work, we find that a module scale system is *economically optimized* with P^* values close to 0.5. Lastly, ε is the effectiveness which is defined as [25]:

$$\varepsilon = \frac{\text{RR}}{\text{RR}_{\text{max}}} \tag{11}$$

where RR is the recovery ratio.

This parameter quantifies whether the PRO module behaves similarly to a one dimensional or a zero dimensional (coupon-sized system). For an infinitely long PRO module ε will be close to 1, while a coupon-sized system will have ε close to 0. The optimized system designs (ε ranging from 0.28 to 0.39) are short with a number of parallel modules, but they are much longer than typical coupon sizes systems.

3.6. Potential ways to further reduce the LCOE

One of the main conclusions of this study is that the draw salinity is the most important parameter in reducing the LCOE and that high draw salinity should be utilized for PRO's economic viability. There are secondary effects which can reduce the LCOE, however. First, economies of scale can reduce the LCOE (i.e., a larger system will have a smaller CapEx per unit membrane area). By increasing the net power output

from 2 MW (the power level used in Sec. 3) to 75 MW, the $\mathrm{LCOE}_{\mathrm{min}}$ reduces by 42%. For a 40 MW net power production[4], the $\mathrm{LCOE}_{\mathrm{min}}$ matches that of wind power at a draw salinity of 18%. Another way to lower the LCOE is by modifying the membrane properties (e.g., membrane structural parameters). It was found that, from an economic perspective, the structural parameter (S) plays a much more important role than the membrane permeability (A) which suffers from strong diminishing returns. These two methods of reducing the LCOE are discussed in detail in Appendix E.

4. Conclusions

A detailed and comprehensive numerical model was developed to study the economic feasibility of PRO for power generation. Whenever there was uncertainty in the selection of model parameters, we made simplifying assumptions which minimized the LCOE. An economic analysis was performed to calculate LCOE and OCC such that the merits of PRO can be directly compared to other sources of power generation including renewables such as wind or solar power. In this work, we chose wind power as a benchmark because of its low LCOE and wide-spread implementation. Our primary conclusions are as follow:

- An optimal condition for the specific power significantly differs from an economic optimum. Therefore, economic analysis must be used to determine the viability of PRO.
- CapEx is the largest constituent factor of $\mathrm{LCOE}_{\mathrm{min}}$, which decreases drastically with increasing draw salinity. Therefore, energetic considerations alone cannot determine viability of PRO.
- High draw salinities lead to relatively lower pretreatment energy costs. Therefore, there is more flexibility in the choice of the draw stream source when high salinity streams are used.
- High hydraulic pressure is an engineering challenge for a high draw salinity operation. An $\mathrm{LCOE}_{\mathrm{min}}$ of \$0.094/kWh can be attained with more a more manageable, but non-optimal, pressure of 83 bar (maximum rated operating pressure of commercial RO membranes) for a 2 MW plant using 0.1/26% salinity pair.
- Future membrane research should focus on reducing the structural parameter (S) rather than increasing the membrane water permeability (A).

5. Acknowledgement

The authors would like to thank Kuwait Foundation for the Advancement Sciences (KFAS) for their financial support through Project No. P31475EC01. LDB acknowledges that this material is based upon work supported by the National Science Foundation Graduate Research Fellowship Program under Grant No. 1122374.

[4]The maximum permeation rate is constrained at 250,000 m^3/day which is the maximum permeation rate available in Desaldata.com [31]. At 40 MW, 18% draw salinity resulted in 250,000 m^3/day.

References

[1] S. Hastings-Simon, D. Pinner, M. Stuchtey, Myths and realities of clean technologies (2014).

[2] S. Chu, A. Majumdar, Opportunities and challenges for a sustainable energy future, Nature 488 (7411) (2012) 294–303.
URL http://dx.doi.org/10.1038/nature11475

[3] R. Pattle, Electricity from fresh and salt water-without fuel, Chemical Process and Engineering 35 (1955) 351–354.

[4] S. Loeb, Osmotic power plants, Science 189 (1975) 654–655.

[5] S. Loeb, Method and apparatus for generating power utilizing reverse electrodialysis, US Patent 4,171,409 (Oct. 16 1979).
URL https://www.google.com/patents/US4171409

[6] J. G. Hong, W. Zhang, J. Luo, Y. Chen, Modeling of power generation from the mixing of simulated saline and freshwater with a reverse electrodialysis system: The effect of monovalent and multivalent ions, Applied Energy 110 (2013) 244 – 251. doi:10.1016/j.apenergy.2013.04.015.
URL http://www.sciencedirect.com/science/article/pii/S0306261913003097

[7] A. Daniilidis, R. Herber, D. A. Vermaas, Upscale potential and financial feasibility of a reverse electrodialysis power plant, Applied Energy 119 (2014) 257 – 265. doi:10.1016/j.apenergy.2013.12.066.
URL http://www.sciencedirect.com/science/article/pii/S0306261914000142

[8] A. M. Weiner, R. K. McGovern, J. H. Lienhard V, A new reverse electrodialysis design strategy which significantly reduces the levelized cost of electricity, Journal of Membrane Science 493 (2015) 605 – 614. doi:10.1016/j.memsci.2015.05.058.
URL http://www.sciencedirect.com/science/article/pii/S0376738815004962

[9] J. W. Post, J. Veerman, H. V. Hamelers, G. J. Euverink, S. J. Metz, K. Nymeijer, C. J. Buisman, Salinity-gradient power: Evaluation of pressure-retarded osmosis and reverse electrodialysis, Journal of Membrane Science 288 (1–2) (2007) 218 – 230. doi:10.1016/j.memsci.2006.11.018.
URL http://www.sciencedirect.com/science/article/pii/S0376738806007575

[10] J. Maisonneuve, C. B. Laflamme, P. Pillay, Experimental investigation of pressure retarded osmosis for renewable energy conversion: Towards increased net power, Applied Energy 164 (2016) 425 – 435. doi:10.1016/j.apenergy.2015.12.007.
URL http://www.sciencedirect.com/science/article/pii/S0306261915015731

[11] G. Han, Q. Ge, T.-S. Chung, Conceptual demonstration of novel closed-loop pressure retarded osmosis process for sustainable osmotic energy generation, Applied Energy 132 (2014) 383 – 393. doi:10.1016/j.apenergy.2014.07.029.
URL http://www.sciencedirect.com/science/article/pii/S0306261914007107

[12] W. He, Y. Wang, M. H. Shaheed, Maximum power point tracking (MPPT) of a scale-up pressure retarded osmosis (PRO) osmotic power plant, Applied Energy 158 (2015) 584 – 596. doi:10.1016/j.apenergy.2015.08.059.
URL http://www.sciencedirect.com/science/article/pii/S0306261915009927

[13] J. L. Prante, J. A. Ruskowitz, A. E. Childress, A. Achilli, RO-PRO desalination: An integrated low-energy approach to seawater desalination, Applied Energy 120 (2014) 104 – 114. doi:10.1016/j.apenergy.2014.01.013.
URL http://www.sciencedirect.com/science/article/pii/S0306261914000324

[14] H. Sakai, T. Ueyama, M. Irie, K. Matsuyama, A. Tanioka, K. Saito, A. Kumano, Energy recovery by PRO in sea water desalination plant, Desalination 389 (2016) 52 – 57. doi:10.1016/j.desal.2016.01.025.
URL http://www.sciencedirect.com/science/article/pii/S001191641630025X

[15] R. Kleiterp, The feasibility of a commercial osmotic power plant, Master's thesis, Delft University of Technology (2012).

[16] K. L. Lee, R. W. Baker, H. K. Lonsdale, Membranes for power generation by pressure-retarded osmosis, Journal of Membrane Science 8 (2) (1981) 141 – 171. doi:10.1016/S0376-7388(00)82088-8.
URL http://www.sciencedirect.com/science/article/pii/S0376738800820888

[17] G. Z. Ramon, B. J. Feinberg, E. M. V. Hoek, Membrane-based production of salinity-gradient power, Energy & Environmental Science 4 (2011) 4423–4434. doi:10.1039/C1EE01913A.
URL http://dx.doi.org/10.1039/C1EE01913A

[18] S. E. Skilhagen, J. E. Dugstad, R. J. Aaberg, Osmotic power — power production based on the osmotic pressure difference between waters with varying salt gradients, Desalination 220 (1–3) (2008) 476 – 482, european Desalination Society and Center for Research and Technology Hellas (CERTH), Sani Resort 22 –25 April 2007, Halkidiki, GreeceEuropean Desalination Society and Center for Research and Technology Hellas (CERTH), Sani Resort. doi:10.1016/j.desal.2007.02.045.
URL http://www.sciencedirect.com/science/article/pii/S0011916407006467

[19] G. Wetterau, Desalination of Seawater: M61, AWWA Manual of Practice, American Water Works Association, 2011.
URL https://books.google.com/books?id=M3W7QsfdyMIC

[20] S. Loeb, Energy production at the Dead Sea by pressure-retarded osmosis: challenge or chimera?, Desalination 120 (3) (1998) 247 – 262. doi:10.1016/S0011-9164(98)00222-7.
URL http://www.sciencedirect.com/science/article/pii/S0011916498002227

[21] http://data.bls.gov/cgi-bin/cpicalc.pl (2016).

[22] S. Loeb, One hundred and thirty benign and renewable megawatts from Great Salt Lake? the possibilities of hydroelectric power by pressure-retarded osmosis, Desalination 141 (1) (2001) 85 – 91. doi:10.1016/S0011-9164(01)00392-7.
URL http://www.sciencedirect.com/science/article/pii/S0011916401003927

[23] N. Y. Yip, A. Tiraferri, W. A. Phillip, J. D. Schiffman, L. A. Hoover, Y. C. Kim, M. Elimelech, Thin-film composite pressure retarded osmosis membranes for sustainable power generation from salinity gradients, Environmental Science & Technology 45 (10) (2011) 4360–4369. doi:10.1021/es104325z.
URL http://dx.doi.org/10.1021/es104325z

[24] N. Y. Yip, M. Elimelech, Performance limiting effects in power generation from salinity gradients by pressure retarded osmosis, Environmental Science & Technology 45 (23) (2011) 10273–10282. doi:10.1021/es203197e.
URL http://dx.doi.org/10.1021/es203197e

[25] L. D. Banchik, M. H. Sharqawy, J. H. Lienhard V, Limits of power production due to finite membrane area in pressure retarded osmosis, Journal of Membrane Science 468 (2014) 81 – 89. doi:10.1016/j.memsci.2014.05.021.
URL http://www.sciencedirect.com/science/article/pii/S037673881400386X

[26] Levelized cost and levelized avoided cost of new generation resources in the annual energy outlook 2015, Tech. rep., U.S. Energy Information Administration (2015).

[27] Updated capital cost estimates for utility scale electricity generating plants, Tech. rep., U.S. Energy Information Administration (April 2013).

[28] S. Loeb, Large-scale power production by pressure-retarded osmosis, using river water and sea water passing through spiral modules, Desalination 143 (2) (2002) 115 – 122. doi:10.1016/S0011-9164(02)00233-3.
URL http://www.sciencedirect.com/science/article/pii/S0011916402002333

[29] A. P. Straub, A. Deshmukh, M. Elimelech, Pressure-retarded osmosis for power generation from salinity gradients: is it viable?, Energy & Environmental Science 9 (2016) 31–48. doi:10.1039/C5EE02985F.
URL http://dx.doi.org/10.1039/C5EE02985F

[30] A. P. Straub, S. Lin, M. Elimelech, Module-scale analysis of pressure retarded osmosis: Performance limitations and implications for full-scale operation, Environmental Science & Technology 48 (20) (2014) 12435–12444. doi:10.1021/es503790k.
URL http://dx.doi.org/10.1021/es503790k

[31] Global Water Intelligence, https://www.desaldata.com/ (2015).

[32] A. P. Straub, N. Y. Yip, M. Elimelech, Raising the bar: Increased hydraulic pressure allows unprecedented high power densities in pressure-retarded osmosis, Environmental Science & Technology Letters 1 (1) (2014) 55–59. doi:10.1021/ez400117d.
URL http://dx.doi.org/10.1021/ez400117d

[33] S. A. Klein, Engineering Equation Solver.

[34] R. A. Robinson, R. H. Stokes, Electrolyte solutions, 2nd Edition, Dover Publications, 2002.

[35] Energy Information Administration (EIA), https://www.eia.gov (accessed Dec. 2015).

[36] DOW FILMTEC Membranes, SW30HR-380 High Rejection Seawater Reverse Osmosis Element Product Manual, DOW (2013).

[37] DOW FILMTEC Membranes, SW30XHR-440i Seawater Reverse Osmosis Element Product Manual, DOW (2013).
URL http://msdssearch.dow.com/PublishedLiteratureDOWCOM/dh_0894/0901b80380894b72.pdf?filepath=liquidseps/pdfs/noreg/609-03002.pdf&fromPage=GetDoc

[38] Nitto Denko - Hydranautics, Hydranautics Membrane Brochure, Nitto Denko - Hydranautics (2002).
URL http://www.membranes.com/pdf/HYDRABrochure.pdf

[39] TORAY Membranes, TM800M Standard SWRO Product Manual, TORAY (July 2013).
URL http://www.toraywater.com/products/ro/pdf/TM800M.pdf

[40] C. Fritzmann, J. Löwenberg, T. Wintgens, T. Melin, State-of-the-art of reverse osmosis desalination, Desalination 216 (1–3) (2007) 1 – 76. doi:10.1016/j.desal.2006.12.009.
URL http://www.sciencedirect.com/science/article/pii/S0011916407004250

[41] M. Wilf, L. Awerbuch, C. Bartels, M. Mickley, G. Pearce, N. Voutchkov, The Guidebook to Membrane Desalination Technology : Reverse Osmosis, Nanofiltration and Hybrid Systems Process, Design, Applications and Economics, Balaban Publishers, 2011.

[42] J. L. Gordon, Hydraulic turbine efficiency, Canadian Journal of Civil Engineering 28 (2) (2001) 238–253. doi:10.1139/l00-102.
URL http://www.nrcresearchpress.com/doi/abs/10.1139/l00-102

[43] S. Gossler, E. Murray, High efficiency dc motor with generator and flywheel characteristics, US Patent 5,514,923 (May 7 1996).

[44] K. H. Mistry, R. K. McGovern, G. P. Thiel, E. K. Summers, S. M. Zubair, J. H. Lienhard V, Entropy generation analysis of desalination technologies, Entropy 13 (10) (2011) 1829–1864. doi:10.3390/e13101829.
URL http://www.mdpi.com/1099-4300/13/10/1829

[45] R. K. McGovern, J. P. Mizerak, S. M. Zubair, J. H. Lienhard V, Three dimensionless parameters influencing the optimal membrane orientation for forward osmosis, Journal of Membrane Science 458 (2014) 104 – 110. doi:10.1016/j.memsci.2014.01.061.
URL http://www.sciencedirect.com/science/article/pii/S0376738814000842

[46] G. Schock, A. Miquel, Mass transfer and pressure loss in spiral wound modules, Desalination 64 (1987) 339 – 352. doi:10.1016/0011-9164(87)90107-X.
URL http://www.sciencedirect.com/science/article/pii/001191648790107X

[47] R. K. McGovern, D. McConnon, J. H. Lienhard V, The effect of very high hydraulic pressure on the permeability of reverse osmosis membranes, in: IDA World Congress on Desalination and Water Reuse, IDA Ref. No. IDAWC15 McGovern-51654, San Diego, 2015.
URL http://web.mit.edu/lienhard/www/papers/conf/MCGOVERN_IDA_San_Diego_2015.pdf

[48] K. G. Nayar, M. H. Sharqawy, L. D. Banchik, J. H. Lienhard V, Thermophysical properties of seawater: A review and new correlations that include pressure dependence, Desalination 390 (2016) 1 – 24. doi:10.1016/j.desal.2016.02.024.
URL http://www.sciencedirect.com/science/article/pii/S0011916416300807

[49] A. Dickson, C. Goyet, Handbook of methods for the analysis of the various parameters of the carbon dioxide system in sea water; version 2, U.S. Department of Energy, eds., ORNL/CDIAC-74. (1994).

[50] G. P. Thiel, E. W. Tow, L. D. Banchik, H. W. Chung, J. H. Lienhard V, Energy consumption in desalinating produced water from shale oil and gas extraction, Desalination 366 (2015) 94 – 112, energy and Desalination. doi:http://dx.doi.org/10.1016/j.desal.2014.12.038.
URL http://www.sciencedirect.com/science/article/pii/S0011916414006857

[51] M. H. Sharqawy, J. H. Lienhard V, S. M. Zubair, Thermophysical properties of seawater: A review of existing correlations and data, Desalination and Water Treatment 16 (1-3) (2010) 354–380. doi:10.5004/dwt.2010.1.
URL http://web.mit.edu/lienhard/www/Thermophysical_properties_of_seawater-DWT-16-354-2010.pdf

[52] K. S. Pitzer, Thermodynamics of electrolytes. I. Theoretical basis and general equations, The Journal of Physical Chemistry 77 (2) (1973) 268–277. doi:10.1021/j100621a026.
URL http://dx.doi.org/10.1021/j100621a026

[53] K. S. Pitzer, J. J. Kim, Thermodynamics of electrolytes. IV. Activity and osmotic coefficients for mixed electrolytes, Journal of the American Chemical Society 96 (18) (1974) 5701–5707. doi:10.1021/ja00825a004.
URL http://dx.doi.org/10.1021/ja00825a004

[54] D. J. Bradley, K. S. Pitzer, Thermodynamics of Electrolytes. 12. Dielectric Properties of Water and Debye-Hückel Parameters to 350° C and 1 kbar, The Journal of Physical Chemistry 83 (12) (1979) 1599–1603.

[55] K. S. Pitzer, J. C. Peiper, R. H. Busey, Thermodynamic Properties of Aqueous Sodium Chloride Solutions, Journal of Physical and Chemical Reference Data 13 (1) (1984) 1–102. doi:10.1063/1.555709.
URL http://scitation.aip.org/content/aip/journal/jpcrd/13/1/10.1063/1.555709

[56] K. S. Pitzer, A thermodynamic model for aqueous solutions of liquid-like density, Reviews in Mineralogy and Geochemistry 17 (1987) 97–142.

[57] J. F. Zemaitis, D. M. Clark, M. Rafal, N. C. Scrivner, Handbook of Aqueous Electrolyte Thermodynamics, Wiley-AIChE, 1986.

[58] A. Bejan, Advanced engineering thermodynamics, 3rd Edition, Wiley, 2006.

[59] Y. A. Cengel, M. A. Boles, Thermodynamics, an engineering approach, 6th Edition, McGrawHill, 2007.

Appendix A. Detailed economic analysis framework

System integration, by combined design of the PRO process and other associated plants, may reduce the cost of the integrated system through a reduction in construction or permitting costs, or by harnessing the economies of scale arising from a larger combined system. But the extent of the cost reduction strongly depends on the specific case, and not enough data is available to generalize the trend. Therefore, in the case of system integration, our analysis simply assumes that the PRO is added to an existing plant (e.g., SWRO or hydraulic fracturing well) such that the cost of the PRO system is independent of any existing plant.

We assume that both a pretreated draw and feed are available (e.g., reverse osmosis desalination brine and treated wastewater effluent). Because these streams are already available, the costs of intake and outfall systems will be smaller than for a regular RO system. In order to be consistent with the lower limit cost estimation, we also exclude the capital expenditures of intake and outfall systems. This is done by using detailed CapEx breakdown data provided by Desaldata.com [31]. These data include the design cost, equipment and material, pressure vessel, pretreatment, intake and outfall systems, pumps, civil engineering, piping and alloys, legal and professional cost, and installation. However, membrane cost is not included in the CapEx. This is because the membranes must be replaced periodically and, therefore, this cost is not amortized over the entire life of the system like other CapEx items. The membrane replacement cost will be included as an operating expenditure later in the section. Each CapEx item from Desaldata.com is given as a function of pure water production capacity of the RO plant ($\$\text{-day}/\text{m}^3$).

Because PRO is not a desalination technology, we compare the price of the two technologies based on membrane area rather than pure water production. This can be done by assuming an average RO flux of 14 $\text{L}/\text{m}^2\text{-hr}$ [40]. By multiplying the CapEx per pure water production capacity by this value of flux and after some straightforward unit conversion, we obtain the CapEx per membrane area in $\$/\text{m}^2$. Figure A.8 shows RO/PRO CapEx versus membrane area and shows that, due to economies of scale, the marginal CapEx with respect to area decreases with increasing membrane area.

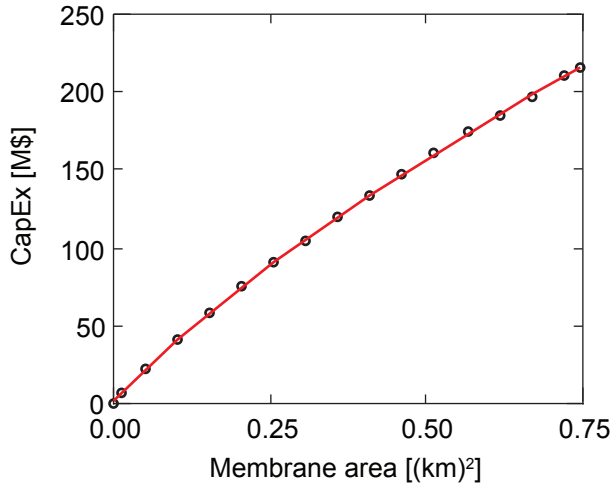

Figure A.8: CapEx as a function of membrane area with a curve fit for system scale reverse osmosis/pressure-retarded osmosis plants. The curve fit equation is $\text{CapEx} = 100.6A_\text{m}^3 - 218.1A_\text{m}^2 + 394.3A_\text{m} + 1.95$ with $R^2 = 1.000$. This CapEx data excludes pretreatment and intake and outfall system.

In order to account for the contribution of CapEx to LCOE_min, the capital recovery factor (CRF) was used. CRF is defined as the ratio of equal annuity (uniform payment made annually) to the present value of the sum of the annuity over the loan period (n). Because CapEx must be payed in year zero, it is the present value by definition. Therefore, the product of CapEx and CRF gives the uniform annual payment incurred due to CapEx which accounts for the interest rate (i). In this work, a 25 year loan period and 8% interest rate were used, again benchmarking RO systems [19]. CRF can be calculated as:

$$\text{CRF} = \frac{i\,(1+i)^n}{(1+i)^n - 1} \tag{A.1}$$

The contribution of CapEx to $\mathrm{LCOE_{min}}$ ($\mathrm{LCOE_{CapEx}}$) can be calculated using Eq. (A.2):

$$\mathrm{LCOE_{CapEx}} = \frac{\mathrm{CapEx} \cdot \mathrm{CRF}}{\dot{W}_{\mathrm{net}} t_{\mathrm{op}}} \tag{A.2}$$

Operating expenditure (OpEx) includes labor, membrane replacement, chemicals, etc. In order to be consistent with the lower limit cost estimation, only membrane replacement is included in the OpEx because other items are not fully understood for PRO application.

The average life of a membrane was assumed to be 4 years [20]. Therefore, 25% of the membrane area is replaced each year [20, 40]. The $\mathrm{LCOE_{min}}$ contribution of membrane replacement cost ($\mathrm{LCOE_m}$) can be calculated using Eq. (A.3):

$$\mathrm{LCOE_m} = \frac{C_{\mathrm{m}} A_{\mathrm{m}}}{L_{\mathrm{m}} \dot{W}_{\mathrm{net}} t_{\mathrm{op}}} \tag{A.3}$$

where C_{m}, A_{m}, L_{m} are cost per unit membrane area, total area, and lifetime of the membrane, respectively, and t_{op} is the amount of hours the plant is running per year. We assume that the plant will operate for 330 days per year (90% capacity factor).

The total $\mathrm{LCOE_{min}}$ can now be calculated by adding the contributions from CapEx and OpEx. Equation (1) is repeated for convenience.

$$\mathrm{LCOE_{min}} = \frac{\mathrm{CapEx} \cdot \mathrm{CRF}}{\dot{W}_{\mathrm{net}} t_{\mathrm{op}}} + \frac{C_{\mathrm{m}} A_{\mathrm{m}}}{L_{\mathrm{m}} \dot{W}_{\mathrm{net}} t_{\mathrm{op}}} \tag{A.4}$$

If $\dot{W}_{\mathrm{PRO}}$ is known, the net power ($\dot{W}_{\mathrm{net}}$) can be calculated using Eq. (3), which in turn can be substituted into Eq. (1) and (2) to calculate $\mathrm{LCOE_{min}}$ and $\mathrm{OCC_{min}}$, respectively.

Appendix B. Detailed model description

The turbine and generator isentropic efficiencies were assumed to be 90% [42, 43]. The pressure exchanger efficiency (η_{PX}) is assumed to be 96% [44]. Equation (B.1) is used to calculate $P_{\mathrm{recovered}}$.

$$P_{\mathrm{recovered}} = P_{\mathrm{in}} + \eta_{\mathrm{PX}} \left(P_{\mathrm{d,out}} - P_{\mathrm{o}} \right) \tag{B.1}$$

The film theory model was used to account for internal and external concentration polarization and salt back diffusion. Yip et al. [23] used these expressions with the van 't Hoff approximation which can significantly underpredict the osmotic pressure at high salinities. At a salinity of 10%, for instance, a linearized osmotic pressure function using a van 't Hoff approximation gives 85 bar, which is a 9% difference from the nonlinear osmotic pressure. In this work, we assume that the membrane is in PRO mode where the membrane's support layer faces the feed solution [45]. We use implicit Eqs. (9) and (10) to relate the concentrations at the membrane surface to those at the bulk on the draw and feed side, respectively. Subsequently, these concentrations are used to evaluate the osmotic pressure, thereby accounting for the non-linear dependence of osmotic pressure on concentration. In the present model, we do not consider concentrative external concentration polarization on the feed side, which is often neglected in computing water and salt transport through asymmetric membranes. This is another assumption that will underpredict the LCOE and OCC.

Viscous pressure drop affects the net driving force for water flux along the flow direction as well as increasing pumping costs. In order to investigate the pressure drop, the geometry of the PRO module must be specified. Since PRO is not a well-established technology, reverse osmosis module parameters were used as a benchmark for geometry selection. Darcy friction factor and mass transfer coefficient correlations (in terms of the Sherwood number) for spacer-filled RO modules were developed by Schock and Miquel [46] and used to calculate viscous pressure drop in the PRO feed and draw streams.

$$f = 6.23 \mathrm{Re}^{-0.3} \tag{B.2}$$

$$\mathrm{Sh} = 0.065 \mathrm{Re}^{0.875} \mathrm{Sc}^{0.25} \tag{B.3}$$

where friction factor is defined as a dimensionless pressure drop,

$$\Delta P = f \frac{1}{2} \rho v^2 \frac{\Delta x}{d_\mathrm{h}} \tag{B.4}$$

and Sherwood number is the dimensionless mass transfer coefficient.

$$k = \frac{\mathrm{Sh} D}{d_\mathrm{h}} \tag{B.5}$$

Equations (B.3) and (B.2) can be substituted into Eqs. (B.4) and (B.5), respectively, to calculate the pressure drop and the mass transfer coefficient.

They also provided an effective hydraulic diameter (d_h) for commercial RO modules. Based on this value, a channel height (h) of 0.75 mm was used for the PRO analysis. A typical RO spiral wound membrane element [41] has about 37 m^2 of membrane area with a length of 1 m. Therefore, a depth (d) of 37 m is chosen for the PRO system. This defines the geometry of one PRO module, and a number of parallel PRO modules are used to scale up the system to meet the specified total power requirement. It is important to note that altering the depth (d) does not alter the power density or the cost because velocities are specified, and the transport characteristics do not depend on the depth. In other words, one large module that has an effective depth of $d_\mathrm{eff} = d \times N_\mathrm{module}$ has the same net power production as N modules each with d; parallel break down of modules is used simply to pile up the module in more compact manner. Figure B.9 shows the PRO module geometry. The total input flow rate of draw stream ($Q_\mathrm{d,in,total}$) is equally divided ($q_\mathrm{d,in} = Q_\mathrm{d,in}/N_\mathrm{module}$) and fed to each module and is likewise done for the feed stream.

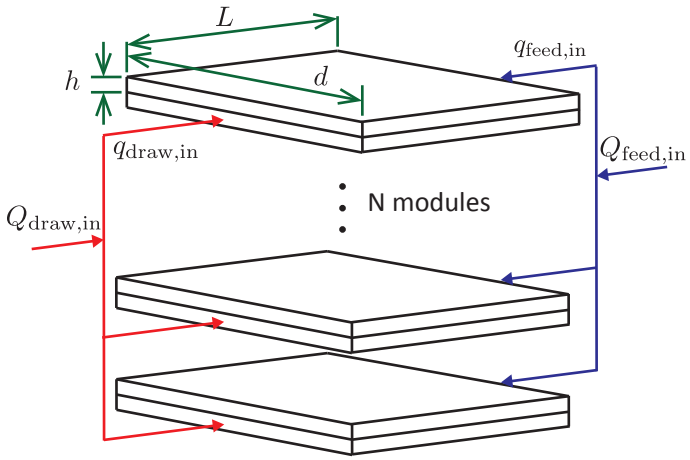

Figure B.9: Parallel module geometry.

When high hydraulic pressures exist on the draw side, the membrane will be compacted. This effect has not been actively studied in the PRO literature mainly because hydraulic pressure is low for pairing seawater and river water. In order to increase the power production or reduce costs, the draw salinity and, correspondingly the hydraulic pressure, should be increased. For saturated NaCl brine and river water pairing, the optimal transmembrane hydraulic pressure can exceed 170 bar, and membrane compaction greatly reduces the membrane permeability. Using experimental data for RO by McGovern et al. [47], the percentage of pure water membrane permeability reduction is calculated. We assume that PRO membranes will be similarly compacted by high pressures given their likeness to RO membranes in terms of materials and design. Only three data points are available, and an exponential curve fit of these was used to prevent over-predicting the compaction for higher pressures. Figure B.10 shows the compaction curve fit in the form of a reduction factor.

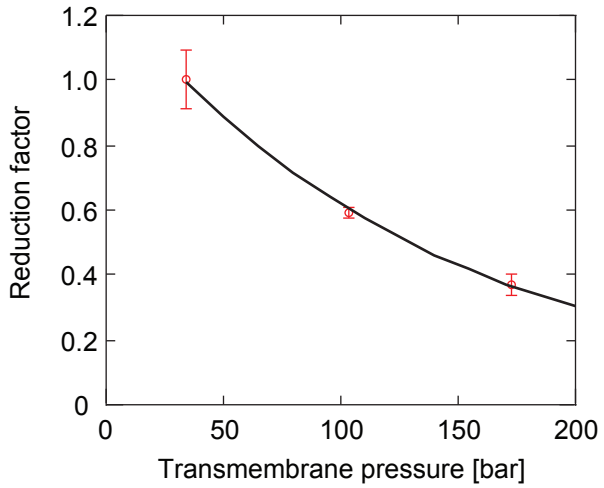

Figure B.10: Membrane permeability reduction factor as a function of transmembrane pressure. Experimental data, points, from McGovern et al. [47]. The curve fit equation is RF $= 1.27\exp(-0.0072\Delta P)$ with $R^2 = 0.999$. The error bar is the range of one standard deviation.

At any location within the PRO module, the membrane permeability was calculated by multiplying the nominal permeability with reduction factor ($A_{\text{compacted}} = A_{\text{nominal}} \cdot \text{RF}$) where RF is the reduction factor.

Appendix C. Pitzer's equations for NaCl solution properties used to approximate seawater properties over a wide salinity range

Seawater properties are available as curve fit equations based on experimentally obtained data, only up to a salinity of 12% [48]. In order to model extremely high salinity draw streams, aqueous NaCl properties are used in this study for both feed and draw streams. Because NaCl contributes a major fraction of total solutes in seawater (sodium and chloride ions contribute 86% of the total solute mass [49]), the NaCl osmotic pressure closely represents seawater and brine streams concentrated from seawater. Furthermore, NaCl solutions accurately model several produced water streams from hydraulic fracturing [50]. We also use Pitzer's equations to determine density as a function of NaCl salinity.

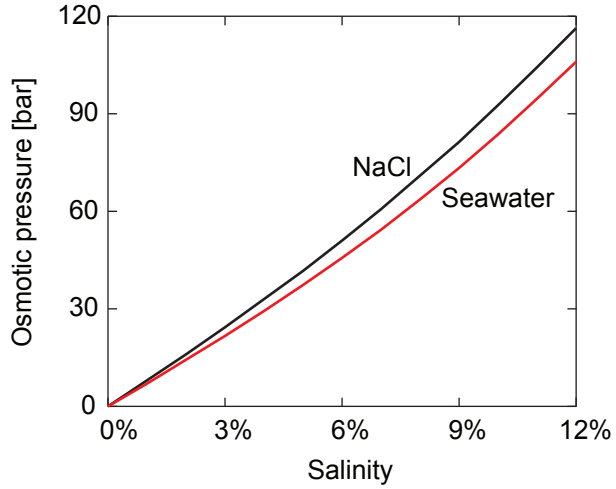

Figure C.11: Osmotic pressure of aqueous NaCl solution and seawater.

Figure C.11 shows the osmotic pressure of NaCl solution and seawater. The seawater properties used are found in Nayar et al. and Sharqawy et al. [48, 51] and the aqueous NaCl solution used is given by Pitzer's

equations [52, 53, 54, 55, 56, 57]. The summary of how to use Pitzer's equation in this context can be found in Appendix A.1 in Thiel et al. [50].

The osmotic pressure of the NaCl solution is higher than that of seawater for a given salinity. By using NaCl properties instead of seawater, the osmotic driving force is slightly over-predicted, which results in an underprediction of LCOE and OCC. The choice of using NaCl feed and draw streams, therefore, is consistent with our aim to estimate a minimum LCOE and OCC for pressure-retarded osmosis.

Appendix D. Dependence of power production on the feed salinity

For reversible salinity gradient power systems [58, 59] and pressure-retarded osmosis, power production depends more upon the salinity ratio than the difference. Therefore a lower salinity feed stream has a more important role in maximizing the power production. Below, we demonstrate the mathematical dependence of power production on feed salinity in large-scale irreversible PRO.

From Banchik et al. [25], the maximum power of an irreversible, counterflow PRO system is obtained when system size tends towards infinity and the mass flow rate ratio, MR, is large. For these limits, the power production per unit of feed flow rate can be shown to be

$$E_{\mathrm{PRO}} = \frac{\rho_{\mathrm{f,in}}}{\rho_{\mathrm{d,out}}} \frac{\eta}{3600} \pi_{\mathrm{f,in}} \left(\sqrt{\frac{\pi_{\mathrm{d,in}}}{\pi_{\mathrm{f,in}}}} - 1 \right)^2 \tag{D.1}$$

according to Banchik et al. [25], after dividing by $\Delta\pi_{\max} \cdot \pi_{\mathrm{f}}$ and performing some mathematical rearrangement. Here, η is the combined isentropic efficiency of the turbine and generator. Equation D.1 is viewed as an upper bound estimate of power production because it is derived assuming that there is no reverse salt flux, viscous pressure drop, concentration polarization, or change in the membrane water permeability. In addition, the pressure exchanger and pump are assumed to operate in an isentropic manner. Table D.4 shows how E_{PRO} is affected by changing the salinity pair. In all cases, the salinity difference is maintained at 3.5%. Clearly a low feed salinity results in significantly higher E_{PRO} for a given salinity difference.

Table D.4: Specific energy (E_{PRO}) of salinity pairs whose salinity differences are 3.5%.

Salinity pair	E_{PRO} [kWh/m^3]
0/3.5%	0.7359
3.5/7%	0.1509
7/10.5%	0.1018
10.5/14%	0.0841

Referring back to Eq. D.1, to maximize E_{PRO}, lower feed osmotic pressure ($\pi_{\mathrm{f,in}}$), or upon invoking the van 't Hoff relation, lower feed salinity $w_{\mathrm{f,in}}$ should be used.

Appendix E. Decreasing the structural parameter (S) and harnessing economies of scale can further reduce the $\mathrm{LCOE}_{\mathrm{min}}$

While increasing the draw salinity is the most effective way to reduce the $\mathrm{LCOE}_{\mathrm{min}}$, exploiting economies of scale and improving membrane properties can even further reduce the $\mathrm{LCOE}_{\mathrm{min}}$. In this section, we investigate each method.

From the results of Sec. 3.2, the draw salinity should be extremely high in order for the $\mathrm{LCOE}_{\mathrm{min}}$ and $\mathrm{OCC}_{\mathrm{min}}$ of PRO to be comparable to wind power. Therefore, we focus on a 0.1/26% salinity combination. Because the CapEx was found to be the major cost factor, harnessing economies of scale could be an effective way to further lower the LCOE. In this section, the net power production is varied from 2 MW (the net power output used in Sec. 3.2) to 75 MW to quantify the cost reduction achievable from economies of scale.

Figure E.12 shows the $\mathrm{LCOE}_{\mathrm{min}}$ and its constituent parts. When the net power is increased from 2 MW to 75 MW, the $\mathrm{LCOE}_{\mathrm{min}}$ decreases by 42%! This significant reduction is possible because CapEx is the dominant cost factor, and economies of scale directly affect the CapEx. Although $\mathrm{LCOE}_{\mathrm{min}}$ is lower than

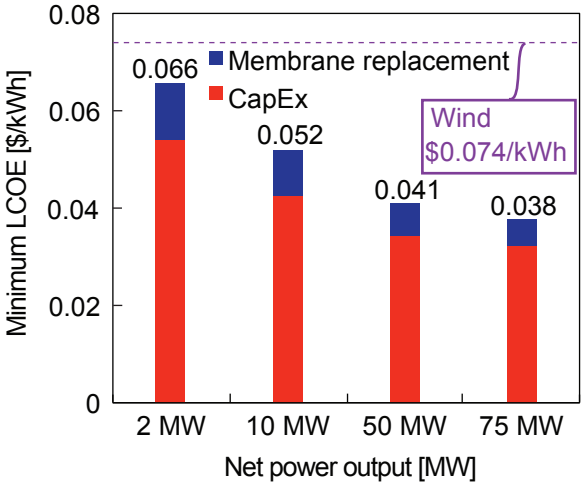

Figure E.12: Effect of plant size on LCOE_{min} for a 0.1/26% salinity pair.

that of wind for power output greater than 10 MW, the economic viability is not guaranteed because of the many assumptions we made which resulted in a minimum LCOE. This result does show, however, that PRO has the potential to be economically viable only for extreme salinity operation such as the 0.1/26% pair [5]. To be more specific, a draw salinity of at least 18% is needed for the minimum LCOE to be comparable to that of wind while harnessing economies of scale. Also there exist diminishing returns on the effect of economies of scale so that increasing the system size does not indefinitely reduce the LCOE.

Modifying the membrane properties can also reduce the LCOE_{min}. Previous results were based on a commercially available FO membrane. Here, we investigate the potential LCOE_{min} reduction from advancement in membrane research. From this, we can identify the proper direction for future membrane research.

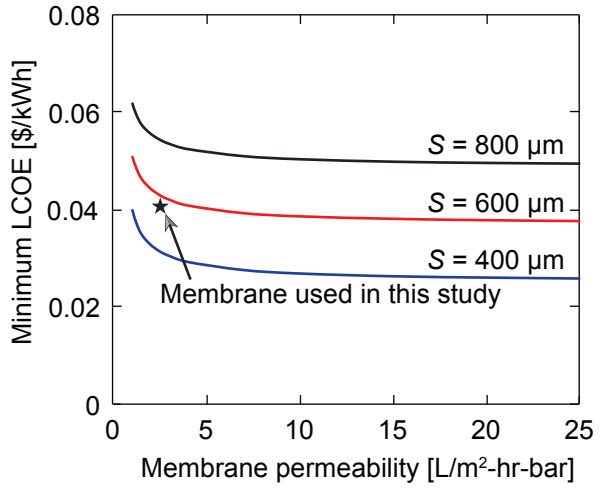

Figure E.13: Effect of membrane permeability (A) and structural parameter (S) on LCOE_{min} while holding the salt rejection coefficient (B) constant (0.1% and 26% salinity pair at 50 MW net power output). The star represents the commercial membrane used in this study, with $A = 2.49$ L/m^2-hr-bar, $B = 0.39$ L/m^2-hr and $S = 564$ μm.

Figure E.13 shows LCOE_{min} as a function of membrane permeability (A) for three different values of S.

[5] For the 0.1/26% salinity pair with 75 MW of net power production, the OCC_{min} value matches that of wind power, with \$2.2/MW.

In general, B increases with A, and increased permeability does not guarantee improved performance. The degree to which B increases with increasing A depends on the membrane, and any projection is subject to error. Instead, B is held constant, to ensure a lower limit estimate of LCOE. The same membrane price ($\$15/m^2$) as RO membranes is used in this analysis. This assumes that the hypothetical membranes can be manufactured at the current price of RO membranes. Even with these assumptions, $LCOE_{min}$ decreases only by 9% when A is increased ten fold from 2.5 to 25 L/m^2-hr-bar with $S = 800$ μm. Strong diminishing returns exist due to concentration polarization, and increasing the membrane permeability is not sufficient to decrease $LCOE_{min}$ significantly. Decreasing S results in a much larger reduction in $LCOE_{min}$. For example, when S is reduced from 800 to 400 μm, $LCOE_{min}$ is decreased by about 44%. This is because S is directly related to internal concentration polarization (ICP) in the support layer, which is the dominant factor reducing the driving force for water flux [16, 25]. The effect of S will be even more pronounced in reality because this analysis neglected the permeability-selectivity tradeoff (i.e. B increases with A) so that the effect of increasing A on reducing the $LCOE_{min}$ is overpredicted. Therefore, future membrane development should focus on reducing S in an attempt to minimize the LCOE.